ELSEVIER

Biophysical Chemistry 109 (2004) 351–360

Biophysical Chemistry

www.elsevier.com/locate/bpc

Characterization of the photoproducts of protoporphyrin IX bound to human serum albumin and immunoglobulin G

Lorenzo Brancaleon[a,*], Steven W. Magennis[b], Ifor D.W. Samuel[b], Ebinazar Namdas[b], Andrea Lesar[a], Harry Moseley[a]

[a]*The Scottish PDT Centre, Department of Dermatology and Photobiology Unit, Ninewells Hospital and Medical School, Dundee, UK*

[b]*Organic Semiconductor Centre, School of Physics and Astronomy, University of St. Andrews, St. Andrews, UK*

Received 2 September 2003; received in revised form 17 December 2003; accepted 19 December 2003

Abstract

Clinically useful photosensitisers (PSs) are likely bound to subcellular and molecular targets during phototherapy. Binding to a macromolecule has the potential to change the photophysical and photochemical characteristics of the PSs that are crucial for their phototoxicity and cell-killing activity. We investigated the effects of binding of a specific PS (protoporphyrin IX or PPIX) to two proteins, human serum albumin (HSA) and a commercially available immunoglobulin (IgG). These two proteins provide two different environments for PPIX. The albumin binds PPIX in hydrophobic binding sites located in subdomain IIA and IIIA, conversely IgG leaves PPIX exposed to the solvent. We show that photophysical parameters such as emission maxima and fluorescence lifetime depend on the binding site. Our results indicate that the different binding site yields very different rates of formation of photoproducts (more than three times higher for PPIX bound to HSA than to IgG) and that different mechanisms of formation may be occurring. Our characterization shows the relevance of protein binding for the photochemistry and ultimately the phototoxicity of PSs.
© 2003 Elsevier B.V. All rights reserved.

Keywords: Human serum albumin; Immunoglobulin G; Protoporphyrin IX; Fluorescence spectroscopy

1. Introduction

Protein–photosensitiser interactions are relevant to several areas of photodynamic therapy (PDT). Protein binding may (a) affect the photophysics of PSs (which affects the optimal irradiation wavelength and the quantum yields of the relaxation processes) and (b) affect the photochemistry of PSs (which can modify the production of cytotoxic species). Several proteins have been shown to be direct targets for PDT [1–6]. Hence, it is important to characterize the effects that proteins have on the photophysics and photochemistry of PSs. The photophysical properties of porphyrin-like photosensitisers, e.g. PPIX, depend strongly on the environment surrounding the tetrapyrrolic ring [7–

Abbreviations: PS, photosensitisers; HSA, human serum albumin; IgG, immunoglobulin G; PDT, photodynamic therapy; PPIX, protoporphyrin IX

*Corresponding author. *Present address*: Department of Physics and Astronomy, University of Texas at San Antonio, 6900 N Loop 1604 W, San Antonio, TX 78249, USA. Tel.: +1-210-458-5694; fax: +1-210-458-4919.

E-mail address: lbrancaleon@utsa.edu (L. Brancaleon).

0301-4622/04/$ - see front matter © 2003 Elsevier B.V. All rights reserved.
doi:10.1016/j.bpc.2003.12.008

11]. Binding to proteins is therefore expected to play a major role in modifying the optical and photochemical properties of PPIX depending on the environment provided by the binding site and the proximity of specific amino acids [12].

Effects of protein binding on PPIX photophysics and photochemistry can be investigated through the characterization of the formation of photoproducts. Photoproducts are formed upon exposure of solutions containing PPIX, to visible light. Although the formation of PPIX photoproducts is not always correlated to PDT efficacy in vivo [13], detection of photoproducts in vitro is indicative of the PSs photochemical activity [14]. We have therefore characterized the formation of the photoproducts of PPIX bound to HSA and IgG. These two proteins are good models for the investigation of the effects of proteins on PSs because they provide two opposite environments. HSA carries two hydrophobic sites located in subdomain IIA and IIIA [7,15]. However, we have previously shown that binding to IgG leaves PPIX exposed to the solvent [15].

In this study we have characterized the differences in the rates and pathway of formation of PPIX bound to albumin and IgG and quantified some important, but often neglected, photophysical parameters of the photoproducts.

2. Materials and methods

2.1. Chemicals

PPIX disodium salt, HSA, IgG immunoglobulin (secondary antibody specific for the α-chain of human IgA) and UV spectroscopy-grade solvents were purchased from Sigma Chemical Co. (Poole, UK) and used as received. For experiments in buffer solution, PPIX was first dissolved in DMSO. This solution was then diluted in buffer to give the final concentration of PPIX in aqueous solution. The maximum final concentration of DMSO in buffer was 5%. Double distilled water was used for the preparation of buffer solutions. Concentration of PPIX was kept near 1 μM and was determined from absorption spectra using a value of $\varepsilon = 2.42 \times 10^5$ (M^{-1} cm^{-1}) at 406 nm [15]. Protein concentration was also determined spectroscopically from the absorption value at 280 nm. Values of ε_{280} for HSA and BSA were obtained from the literature [7] while for IgG we used the value offered by the manufacturer ($\varepsilon_{280} =$ 1400 M^{-1} cm^{-1}). All aqueous solutions were prepared in 10 mM phosphate buffer at pH 7.5.

For experiments in organic solvents PPIX was directly diluted to concentration in the 0.5–1 μM range.

2.2. Steady state fluorescence experiments

A Hitachi F-2500 spectrofluorimeter (Hitachi Instrument Inc., Wokingham Berkshire, UK) was used for all the measurements. All PPIX emission spectra presented in this manuscript were excited at 410 nm and collected with 2.5 nm resolution at a speed of 300 nm/min. Protein intrinsic fluorescence was recorded with excitation at 290 nm. Excitation spectra were recorded with emission wavelength set at the maximum of either PPIX or photoproduct emission. All emission spectra were corrected for the instrumental response.

2.3. Formation of photoproducts

Photoproducts were formed by irradiating the solutions at 630 nm at increasing absorption doses up to 30 J per μM of PPIX. We decided to use the absorption doses rather than irradiation doses in order to normalize the data to the actual amount of light absorbed by each sample. This is justified by the fact that only the light actually absorbed by the sample is responsible for the formation of photoproducts. Irradiation was carried out using a diode laser (PDT 630, Diomed Ltd., Cambridge, UK) coupled to a Microlens fiber (Medlight SA, Ecublens, Switzerland). Before irradiation, the output of the fiber was monitored using a power meter (Ophir 03A, BFI Optilas, Milton Keynes, UK). Irradiation was carried out at radiant power levels of 0.1, 0.5 and 1 W. The presence of photoproducts was periodically monitored during irradiation by recording the emission spectra of the irradiated solutions (excitation at 410 nm).

Since experiments were carried out in aerated solution, we assume that the formation of photoproducts is oxygen dependent [16]. Under this

assumption, the transformation of PPIX molecules into photoproducts produces a decrease in PPIX fluorescence (as PPIX molecules disappear) and an increase in the fluorescence of photoproducts (as photoproduct molecules appear). We can therefore assume that the rate of decrease of the PPIX emission maximum equals the rate of increase of photoproduct fluorescence. Since we assume a limitless supply of oxygen, the decease of PPIX fluorescence will, at least initially, follow a pseudo-first order equation

$$-\mathrm{d}[\mathrm{PP}]/\mathrm{d}E = K_{\mathrm{ph}}[\mathrm{PP}] \quad (1)$$

where K_{ph} is the 'rate' of photoproduct formation, [PP] is the concentration of PPIX and E is expressed as the energy delivered to the solution at 630 nm per μmol of PPIX.

Imposing the boundary condition that $[\mathrm{PP}]_0$ is the initial concentration of PPIX ($E=0$), integration of Eq. (1) leads to:

$$[\mathrm{PP}] = [\mathrm{PP}]_0 \exp(-K_{\mathrm{ph}}E) \quad (2)$$

or

$$\ln([\mathrm{PP}]/[\mathrm{PP}]_0) = -K_{\mathrm{ph}}E \quad (3)$$

Since at the concentration used in our experiments the fluorescence ($\mathrm{F_{IX}}$) of PPIX can be represented as

$$\mathrm{F_{IX}} = k\ \Phi\ [\mathrm{PP}]$$

where k is an instrumental constant and Φ is PPIX fluorescence quantum yield, Eq. (3) can be expressed as

$$\ln(\mathrm{F_{IX}}/\mathrm{F_{IX}^0}) = -K_{\mathrm{ph}}\ E \quad (4)$$

where $\mathrm{F_{IX}^0}$ is the initial PPIX fluorescence intensity.

We established that 30 J/μmol is the irradiation dose where, under our experimental conditions, we reached saturation of photoproduct formation. Based on the results obtained from our studies on binding of PPIX [15], the experiments were carried out at a PPIX/protein molar ratio of approximately 5.

2.4. Fluorescence lifetime

Lifetime measurements were performed using time-correlated single photon counting. The solution samples were measured in a 1 cm pathlength cuvette and were degassed with O_2-free nitrogen. Samples were excited using a pulsed diode laser head ($\lambda_{ex}=393$ nm) and driver (PDL 800-B) from Picoquant (Berlin, Germany), with a repetition rate of 5 MHz. The mean power was ca. 0.1 mW. The emission from the sample was collected at right angles to the excitation, passed through an appropriate longpass filter (Schott KV filters) and then through a f3 monochromator. The light was detected by a Hamamatsu MCP-PMT (R3809U-50) (Welwyn Garden City, England, UK). The instrument response of the system, measured using a Ludox scatterer was approximately 150 ps FWHM. The collected data [$F(t)$] were analyzed using DAS 6 software from IBH (Glasgow, Scotland, UK) by iterative re-convolution of the instrument response with a sum of exponentials

$$F(t) = \sum\nolimits_i \alpha_i \mathrm{e}^{-t/\tau i} \quad (5)$$

where i represents the i-th exponential component with amplitude α_i and lifetime τ_i.

The relative weight of each component is:

$$A_i = \alpha_i\tau_i/(\sum\nolimits_i \alpha_i\tau_i) \quad (6)$$

From these parameters the average lifetime of a decay can be expressed as:

$$\langle\tau\rangle = \sum\nolimits_i A_i\tau_i \quad (7)$$

The quality of the fit was determined by the value of the reduced chi-squared statistical parameter and by visual inspection of residuals. The accuracy of the decay parameters was estimated from at least three separate experiments.

Fluorescence decay of PPIX in irradiated and non-irradiated solutions was investigated throughout the emission spectrum from approximately 590 to 720 nm by changing the central wavelength of the emission monochromator. Fluorescence decays

Table 1
Emission and excitation maxima of PPIX and its photoproducts in different solvents[a]

Solvent	Dielectric constant	Emission Max. of PPIX (nm)	Excitation Max. of PPIX (Soret band) (nm)	Emission Max. of photoproduct (nm)	Excitation Max. of photoproduct (Soret band) (nm)
Buffer (pH 7.4)	80	622	398	651	395
DMSO	47.2	634	408	656	404
Acetonitrile	36.6	633	403	669	400
Methanol	33	634	396	670	386
Acetone	20.7	634	402	672	399
Methanol	20.1	636	398	–	–
Ether	4.3	636	401	–	–
Chloroform	2.24	636	406	675	391
HAS	–	636	412	652	402
	–	–	–	666	402
IgG	–	623	402	669	400

[a] Emission spectra were obtained with excitation at 410 nm. Excitation spectra were recorded with the emission fixed at the emission maximum of PPIX or its photoproducts.

were detected at 10 nm increments from the emission maximum of PPIX. The bandwidth was set between 4 and 6 nm.

3. Results

In general, irradiation of PPIX in solution produces a decrease of the main PPIX fluorescence peak (between 622 and 636 nm depending on the solvent and the protein present in solution [15]) and a correlated increase of one or more peaks in the region between 650 and 680 nm. The peaks appearing in this region are due to PPIX photoproducts [17].

3.1. PPIX in buffer and organic solvents

Steady state fluorescence. There is a large difference between the spectral position of the emission maxima of PPIX and its photoproducts in water and all organic solvents. The emission peak of PPIX shifts from 622 nm in buffer (pH 7.4) to above 634–636 nm in organic solvents (Table 1 and Fig. 1a–c). However, within organic solvents of very different polarity and with very different reactive groups, the shift of the PPIX fluorescence maximum is minimal (Table 1). The position of the emission peak of the photoproducts appears instead to correlate better with the polarity of the environment (Table 1). The photoproduct of PPIX in buffer (pH 7.4) shows a peak near 651 nm, this peak shifts to 656 nm for PPIX in DMSO (Fig. 1a, c). For PPIX in other organic solvents the position of the peak ranges between 670 and 676 nm with decreasing dielectric constant of the solvent (Table 1). Also, the maxima of the excitation spectra do not seem to show a distinct correlation with solvent polarity (Table 1).

Fluorescence decay of non-irradiated solutions. The fluorescence lifetime of PPIX depends on the solvent and on the emission wavelength. At the emission maximum of PPIX the decay in organic solvents is monoexponential with lifetime ranging from 10.8 to 16.8 ns (Fig. 2a and Table 2). There is an apparent increase of the fluorescence lifetime with the polarity of the solvent. In the spectral region between 650 and 680 nm (where in irradiated solution the maxima of photoproducts are found) PPIX shows a quasi-monoexponential decay as the long-lived lifetime is accompanied by a shorter lived (1.5–6 ns) component, which, however, only accounts for 2–5% of the fluorescence decay (Table 2). In buffer, however, the decay of PPIX is bi-exponential at all emission wavelength investigated. The lifetime of the short-lived component is longer in the spectral region of the photoproducts (2.6 ns) than at the maximum of PPIX (1.6 ns) as shown by Table 2. The longer-

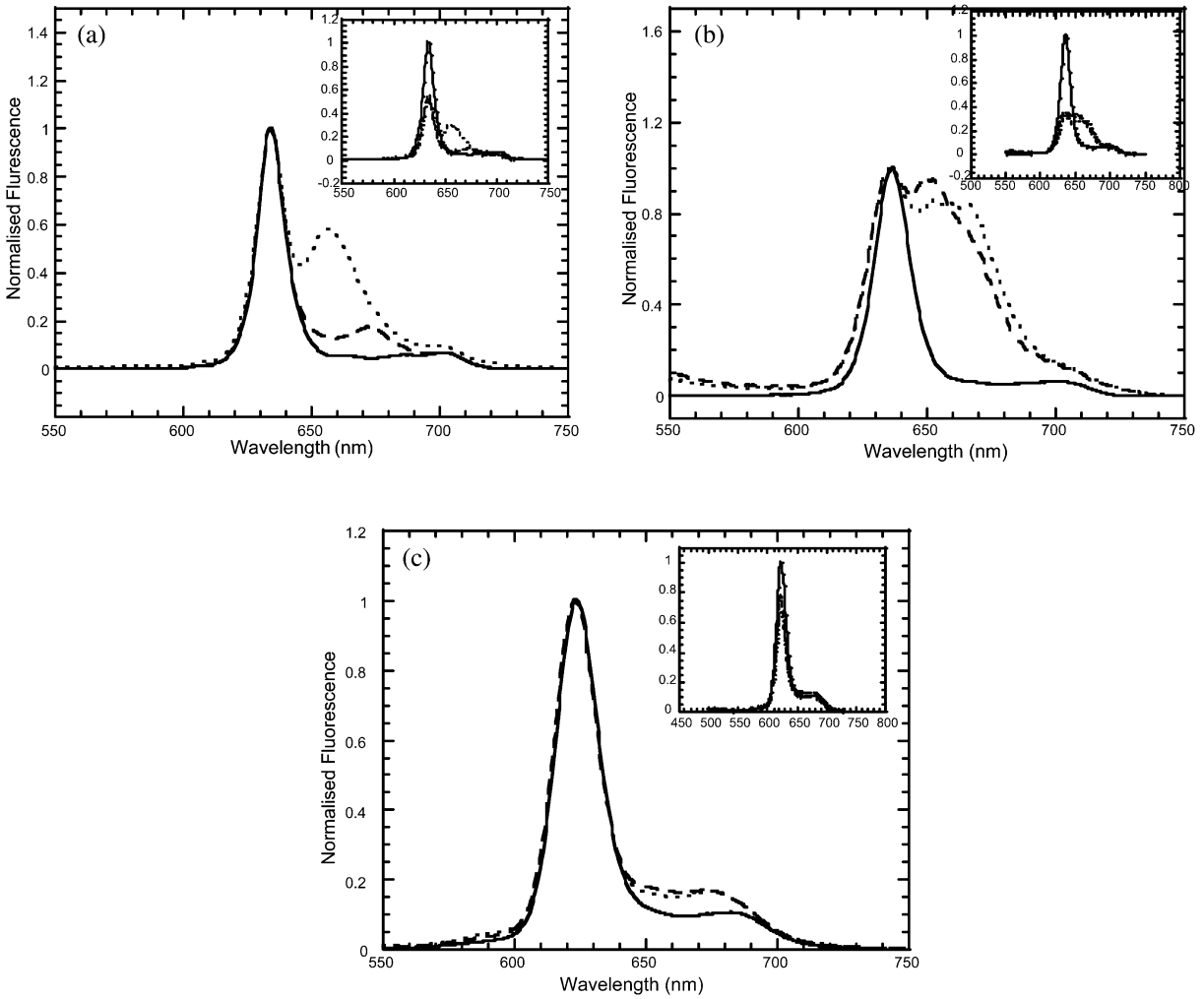

Fig. 1. Normalized emission spectra of photoproducts. The emission spectrum of non-irradiated solutions is represented by the solid line, the spectrum of solutions irradiated for 30 J/μmol at 100 mW is represented by the dashed line, whereas the spectrum of solutions irradiated for 30 J/μmol at 1 W is represented by the dotted line. Spectra are self-normalized to the maximum of PPIX fluorescence. In non-irradiated solutions (solid line), the main emission peak is the maximum of PPIX. In irradiated solutions, the maxima and shoulders at wavelengths longer than the maximum of PPIX are due to photoproducts. (a) PPIX in DMSO; (b) PPIX bound to HSA; (c) PPIX bound to IgG. In the insert of each plot is represented the same set of spectra normalized to the maximum of PPIX fluorescence in the non-irradiated solution. The decrease of the PPIX fluorescence and the increase of the fluorescence of photoproducts can thus be appreciated.

lived component of PPIX in buffer does not correlate with the increased polarity as is the case for PPIX in organic solvents.

Fluorescence decay of irradiated solutions. The fluorescence lifetime of the photoproducts in organic solvents can be detected as an additional decay time (Fig. 2b and Table 3). The lifetime of the photoproducts is intermediate between the short-lived and the long-lived components (Table 3) and ranges between 2.2 and 6.1 ns. Since the

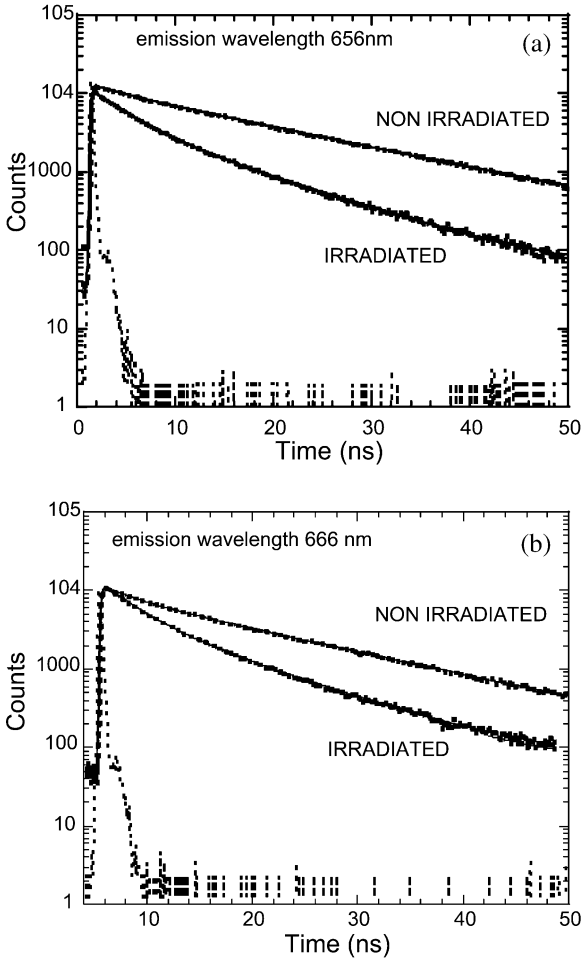

Fig. 2. Fluorescence decay of PPIX and photoproducts. (a) In this figure are represented the fluorescence decay curves of non-irradiated and irradiated solutions of PPIX in DMSO recorded at the wavelength (±4 nm) corresponding to the maximum of photoproduct fluorescence (656 nm). The decay of the non-irradiated solution requires two-component fitting whereas the decay of the irradiated solution requires an additional (third) component. The overall decay is faster (smaller $\langle\tau\rangle$) in the irradiated solution. (b) In this figure are represented the fluorescence decay curves of non-irradiated and irradiated solutions of PPIX bound to HSA recorded at the wavelength (±4 nm) corresponding to the maximum of photoproduct fluorescence (665 nm). The decay of the non-irradiated solution requires two-component fitting whereas the decay of the irradiated solution requires an additional (third) component. The overall decay is faster (smaller $\langle\tau\rangle$) in the irradiated solution.

intermediate component is prevalent the average lifetime $\langle\tau\rangle$ of irradiated solution is shorter (Table 3). The lifetime of the photoproducts formed in organic compounds does not show a correlation with the solvent polarity.

Rate of formation of photoproducts. The initial rate of formation of PPIX photoproducts is linear and can be estimated by fitting the data with Eq. (4). The fitting shows that the formation of photoproducts in DMSO is the second largest among the organic solvents investigated and is 3.3–5.9 larger than in buffer (Table 4 and Fig. 3). Formation is very small in alcohols and acetonitrile (Table 4). The rate of formation in chloroform is an order of magnitude higher than in DMSO.

3.2. PPIX bound to HSA

Steady state fluorescence. Irradiation of PPIX bound to HSA produces two peaks at 652 and 666 nm (Fig. 1b). Excitation spectra of the photoproducts of PPIX bound to HSA recorded with emission at 652 and 666 nm show maxima that are shifted 4–10 nm to shorter wavelengths compared to the maxima of PPIX at the same emission wavelengths. The maximum of the exctiation spectrum of the photoproduct at 652 nm appears at 398 nm whereas the maximum of the photoproduct at 666 nm appears at 404 nm.

Fluorescence decay. In non-irradiated solutions, the decay of PPIX bound to HSA shows a bi-exponential decay both at the emission maximum of PPIX (636 nm) and at the maxima of the two photoproducts (652 and 666 nm) (Table 2). The long-lived component remains identical at the two wavelengths while the short-lived component is slightly faster at the emission wavelength of the photoproducts. In irradiated solutions an intermediate component has to be added to account for the contribution of the photoproduct (Table 3 and Fig. 2b). The lifetime of the intermediate component (6.1 ns) is similar (within experimental error) at 652 and 666 nm and remarkably similar to the value of the photoproduct formed in buffer. The addition of this component results in a shorter average lifetime of PPIX fluorescence decay in the presence of photoproducts (Table 3).

Table 2
Fluorescence decay parameters of PPIX in non-irradiated solutions

Solution	τ_1 (ns)[a]	τ_2 (ns)[a]	A_1 (%)[b]	A_2 (%)[b]	Solvent polarity	Detection wavelength (nm)
DMSO	–	16.8±0.6	–	100	47.2	634
	3.4±0.6	16.8±0.7	4±1	96±3	–	656
Acetointrile	–	15.8±0.5	–	100	36.6	633
	1.5±0.3	15.4±0.6	5±1	95±2	–	669
Methanol	–	13.6±0.5	–	100	33	634
	1±0.4	13.2±0.6	2±1	98±1	–	670
Acetone	–	12.3±0.6	–	100	20.7	634
	1.4±0.3	12±0.8	1	99		672
Propanol	–	13.9±0.9	–	100	20.1	636
	4.6±0.4	13.1±0.5	6±1	94±2	–	670
Ether	–	15.4±0.8	–	100	4.3	636
Chloroform	–	10.2±0.6	–	100	2.2	636
	4.6±0.9	10±0.4	6±1	94±1	–	674
Buffer	1.5±0.4	15.8±0.6	2±1	98±1	80	622
	2.6±0.6	15.4±0.5	10±2	90±2	–	651
With HAS	3.3±0.4	14.5±0.6	2±1	98±1	?	636
	2.7±0.6	14.5±0.6	11±2	89±2	–	666
With IgG	1.4±0.5	15.3±0.5	6±2	94±2	?	623
	2.3±0.4	15.2±0.8	10±3	90±3	–	669

[a] Values calculated from fitting (Eq. (5)).
[b] Values calculated from fitting (Eq. (6)).

Rate of formation of photoproducts. The initial rate of formation of photoproducts (estimated from the linear portion of Fig. 3) is faster than in buffer (5.6–8.9 times faster) and in all organic solvents with the exception of chloroform (Table 4). The rate of formation is identical for the two emission peaks at 652 and 666 nm.

3.3. PPIX bound to IgG

Steady state fluorescence. When PPIX bound to IgG is irradiated, a single peak due to the photoproduct appears at 669 nm (Fig. 1c). This peak occurs at longer wavelength than the one for PPIX bound to albumin. The maximum of the excitation spectrum corresponding to the emission peak of the photoproduct appears at 400 nm.

Fluorescence decay. In non-irradiated solutions, the decay of PPIX bound to IgG shows a bi-exponential decay both at the emission maximum of PPIX (623 nm) and at the maxima of the two photoproduct (669 nm). As was the case for PPIX bound to albumin the long-lived component

Table 3
Fluorescence decay parameters of PPIX in irradiated solutions recorded at the maximum of the emission of the photoproduct

Solution	Lifetime of photoproduct (ns)	Relative contribution of photoproduct to overall decay (%)	Average lifetime before irradiation (ns)	Average lifetime after irradiation (ns)
DMSO	7.5±1.2	67±6	15.9±1	9.7±1.1
Acetonitrile	4.7±0.8	58±3	14.7±1.1	8.8±1.6
Methanol	3.8±1	67±3	13±1	6.6±1.2
Acetone	6.1±1.5	87±7	11.9±1.2	6.8±1.4
Chloroform	2.2±0.8	93±6	9.7±1.1	2.9±1
Buffer	6.2±0.8	33±8	14.1±1.4	10.8±1.2
With HAS	6.1±1.6	49±7	13.2±1.5	8±1.4
With IgG	8.2±1.2	29±8	13.9±1.2	12.5±1.7

Table 4
Values of K_{ph}[a] in 1/J at various irradiance and in different solutions

Solution	Rate of formation of photoproduct (10^{-2} μM/J^{-1})
DMSO	
0.1 W	2.7±0.3
0.5 W	2.8±0.6
1 W	3.6±0.3
Acetonitrile	0.57±0.1
Methanol	0.68±0.1
Acetone	2.1±0.2
Chloroform	0.7±0.2
Buffer	
0.1 W	0.54±0.1
0.5 W	0.86±0.3
1 W	0.61±0.1
With HAS	
0.1 W	4.8±0.1
0.5 W	4.8±0.1
1 W	5.2±0.2
With IgG	
0.1 W	0.8±0.2
0.5 W	1.1±0.1
1 W	0.9±0.2

[a] Values calculated using Eq. (4).

remains identical at the two wavelengths while the short-lived component is slightly longer at the emission wavelength of the photoproducts (Table 2). In irradiated solutions, an intermediate component has to be added to account for the contribution of the photoproduct (Table 3). The lifetime of the photoproduct is longer than the correspondent decay of the photoproduct of PPIX bound to albumin. The presence of this component shortens the average lifetime of the fluorescence decay in the presence of photoproducts (Table 3).

Rate of formation of photoproducts. The rate of formation of the photoproduct (estimated from the linear portion of Fig. 3) is faster (approx. 1.3–1.5 times) than for PPIX in buffer but much slower than the corresponding rate for PPIX bound to albumin or in most organic compounds (Table 4).

4. Discussion

4.1. PPIX bound to HSA

Irradiation of PPIX bound to albumin produces a complex emission spectrum and forms photoproducts at a fairly fast rate (Fig. 1b and Fig. 2). The presence of multiple emission spectra in the region of the photoproducts suggests the presence of multiple products associated with the two main binding sites IIA and IIIA [18]. According to our results in organic solvents, (Table 1) possible site-dependent differences in the polarity of the environment surrounding PPIX could not explain a shift of 14 nm of the emission wavelength (Table 1), even more so if we assume that both main binding sites are hydrophobic. It is therefore reasonable to suggest that the two peaks derive from either two different photoproducts mediated by different proximal amino acids [12] or by the same photoproduct whose emission wavelength is changed by the presence of different proximal amino acids. Further studies, which include the analysis of amino acid degradation have been undertaken to conform this mechanism. The very small decrease in protein fluorescence after irradiation of PPIX (data not shown) suggest only a minimal involvement of tryptophan in photodegradation.

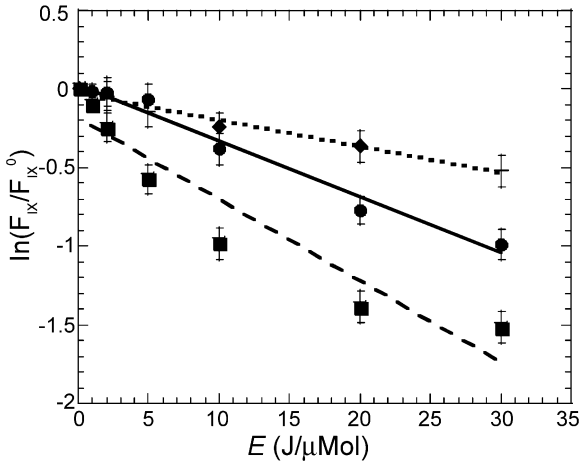

Fig. 3. Dose-dependent formation of photoproducts. Decrease of PPIX fluorescence maximum as a function of E according to Eq. (4). The linearity of the plot ($0.97 < R < 0.99$) confirms the validity of the pseudo-first order model. PPIX in DMSO (circles), PPIX bound to HSA (squares) and PPIX bound to IgG (diamonds). The irradiance was 1 W. The fitting shown was obtained using Eq. (4).

Fluorescence lifetime experiments provide the same lifetime for the photoproduct at 652 and 666 nm (Table 3). This evidence favors the second interpretation as it would have a smaller consequence on the fluorescence lifetime of PPIX. We cannot, however, rule out that the inability to detect a different lifetime for the two photoproducts at 652 and 666 nm which results from the intrinsic limitation of the fluorescence decay deconvolution algorithm.

The rate of photoproduct formation is faster than in any of the solvents investigated (Table 4) with the exception of chloroform. Since our results suggest that there is no correlation between the rate of formation of PPIX photoproducts and the dielectric constant of the solvent (Table 4), we can conclude that the faster rate with HSA is not due to the hydrophobic environment of the protein main binding sites IIA and IIIA. We therefore argue that the proximity of amino acid residues influences the formation of photoproducts. Photoproducts of PPIX bound to albumin may be mediated by singlet oxygen and could involve the reactive group of amino acid side chains [12], however, because of the secluded location of bound PPIX the reactions responsible for the creation of photoproducts could proceed through direct charge transfer with proximal residues (histidine and tryptophan are possible candidates as they participate to the binding site [7,18]). The possibility of this second mechanism would bear great consequences for PDT in vivo as it would introduce a mechanism, which is likely (part of these PSs are likely bound to the hydrophobic sites of proteins) and does not involve production of singlet oxygen which is the fundament of PDT. The bi-exponential decay could also derive from the presence of aggregated forms of PPIX (mostly dimers), which may also bind to the proteins in a mechanism similar to their binding to phospholipids bilayers [11].

4.2. PPIX bound to IgG

Irradiation of PPIX bound to IgG results in a slowly increasing emission peak at 669 nm. The similarity of the fluorescence lifetime parameters of non-irradiated samples (Table 2) confirms our hypothesis that the binding site of IgG leaves the porphyrin exposed to the solvent. The slow rate of photoproduct formation (Table 4) is also consistent with the proximity of the aqueous environment. Other parameters, however, point towards the involvement of proximal amino acids. The fluorescence lifetime of the photoproduct is in fact dissimilar to the one formed in buffer. Moreover, the position of the emission maximum is more in line with the one observed in organic solvents (Table 1). Since we have excluded the possibility that the polarity of the environment is responsible for the spectral position of the photoproducts or for their fluorescence lifetime, once again we suggest that the proximity of certain amino acids influences the formation of the photoproduct. Therefore before irradiation PPIX photophysics is mostly influenced by the aqueous environment, upon irradiation instead, PPIX photochemistry is strongly influenced by the presence of the amino acids in the binding site. From the similarity between the parameters of PPIX photoproduct bound to IgG and those in organic solvents (Tables 1–4) we can also suggest that the mechanism of formation might also be similar and occurring mostly through the reaction with the PPIX triplet-mediated singlet oxygen. This would in turn point to different photochemical mechanisms involved when PPIX is bound to IgG or albumin.

The possibility of protein-dependent photochemical mechanisms would carry important consequences in our understanding of PDT mechanisms.

Acknowledgments

The authors would like to thank the Barbara Stewart Cancer Trust for supporting the Scottish PDT Centre and the Scottish Higher Education Founding Council (SHEFC) for support of the Organic Semiconductor Centre. Prof. Samuel is a Royal Society University Research Fellow.

References

[1] S.L. Gibson, R. Hilf, Interdependence of fluence, drug dose and oxygen on hematoporphyrin derivative induced

photosensitization of tumor mitochondria, Photochem. Photobiol. 42 (1985) 367–373.
[2] J. Morgan, W.R. Potter, A.R. Oseroff, Comparison of photodynamic targets in a carcinoma cell line and its mitochondrial DNA-deficient derivative, Photochem. Photobiol. 71 (2000) 747–757.
[3] C. Berg, J. Moan, Lysosomes and microtubules as targets for photochemotherapy of cancer, Photochem. Photobiol. 65 (1997) 403–409.
[4] K. Boekelheide, J. Eveleth, A.H. Tatum, J.W. Winkelman, Microtubule assembly inhibition by porphyrins and related compounds, Photochem. Photobiol. 46 (1987) 657–661.
[5] L.A. Sporn, T.H. Foster, Photofrin and light induces microtubule depolymerization in cultured human endothelial cells, Cancer Res. 52 (1992) 3443–3448.
[6] D. Kessel, Relocalization of cationic porphyrins during photodynamic therapy, Photochem. Photobiol. Sci. 1 (2002) 837–840.
[7] S.M. Andrade, S.M.B. Costa, Spectroscopic studies on the interaction of a water soluble porphyrin and two drug carrier proteins, Biophys. J. 82 (2002) 1607–1619.
[8] B.M. Aveline, T. Hasan, R.W. Redmond, The effects of aggregation protein binding and cellular incorporation on the photphysical properties of benzoporphyrin derivative monoacid ring A (BPDMA), J. Photochem. Photobiol. B: Biol. 30 (1995) 161–169.
[9] C.Z. Huang, Y.F. Li, N. Li, K.A. Li, S.Y. Tong, Spectral characteristics of αβγδ-tetrakis(*p*-sulfophenyl)porphyrin in the presence of proteins, Bull. Chem. Soc. Jpn. 71 (1998) 1791–1797.
[10] R.F. Pasternack, E.J. Gibbs, D. Bruzewicz, D. Stewart, K.S. Engstrom, Kinetics of disassembly of a DNA-bound porphyrin supramolecular array, J. Am. Chem. Soc. 124 (2002) 3533–3539.
[11] F. Ricchelli, S. Gobbo, G. Moreno, C. Salet, L. Brancaleon, A. Mazzini, Photophysical properties of porphyrin planar aggregates in liposomes, Eur. J. Biochem. 253 (1998) 760–765.
[12] M. Krieg, D.G. Whitten, Self-sensitized photooxidation of protoporphyrin IX and related free-base porphyrin in natural and model membrane systems. Evidence for novel photooxidation pathways involving amino acids, J. Am. Chem. Soc. 106 (1984) 2477–2479.
[13] L. Kunz, A.J. MacRobert, Intracellular photobleaching of 5,10,15,20-tetrakis(*m*-hydroxyphenyl) chlorin (Foscan) exhibits a complex dependence on oxygen level and fluence rate, Photochem. Photobiol. 75 (2002) 28–35.
[14] B.M. Aveline, R.W. Redmond, Can cellular phototoxicity be accurately predicted on the basis of sensitizer photophysics?, Photochem. Photobiol. 69 (1999) 306–316.
[15] L. Brancaleon, H. Moseley, Effects of photoproduct on the binding properties of protoporphyrin IX, Biophys. Chem. 96 (2002) 77–87.
[16] G.S. Cox, D.G. Whitten, Mechanisms for the photooxidation of protoporphyrin IX in solution, J. Am. Chem. Soc. 104 (1982) 516–521.
[17] R.L. Goyan, D.T. Cramb, Near-infrared two-photon excitation of protoporphyrin IX: photodynamics and photoproduct generation, Photochem. Photobiol. 72 (2000) 821–827.
[18] X. Min, D.C. Carter, Atomic structure and chemistry of human serum albumin, Nature 358 (1992) 209–215.